*Geol. Soc. Malaysia, Bulletin 41, December 1997; pp. 139–150*

# Some quantitative studies on wireline logs of the Baram Delta Field

SAHAT SADIKUN

School of Science & Technology
Universiti Malaysia Sabah
Locked Bag 2073
88999 Kota Kinabalu
Sabah

**Abstract:** Some quantitative studies were carried out on nine wells in the Baram Delta Field. Sedimentary cycles boundaries were determined using wireline logs and seismic data. Thicknesses of sand, shaly sand, and shale facies were determined for each well based on gamma ray and spontaneous potential logs. Results showed that the field is sandstone dominated (42.3%). Thicker reservoir sand occurs in Cycle VI Lower which is about 46%. The thickness of this reservoir sand increases toward the north and northwest directions. This reflects that the subsidence of the area increases in these directions. The porosity decreases with depth due to an increase in compaction with depth. The surface porosity is about 60% reaching 20% at a depth of 2,440 m. The shale volume percentage varies from 11.5 for poorly stratified sandstone (Sps), 19 for laminated sandstone (Sl), 33.5 for heterolithic sandstone (Sm) and 77 for mudstone (M) facies. The percentage of density/sonic porosity ranges from 23 for Sps, 22.55 for Sl, 21.45 for Sm and 19.10 for M facies. Rapid sedimentation rates led to the formation of overpressured zone at depth of about 2,100–2,300 m. The geothermal gradient of the area shows an average of 1.75°C/100 m and increases to an average of 2.75°C/100 m at the top of the overpressured zone, a depth of about 2,250 m. The overpressured zone is unfavourable habitat for hydrocarbons.

## INTRODUCTION

Wireline logs are readily available and provide continuous records of the physical characteristics of all the formations crossed by all the wells in a field. Log responses are function of lithology, porosity, fluid content and textural variations. As such, logs are ideal tools for quantitative evaluation of the fluid content of each potential reservoir, and orientation of reservoirs. Wireline logs also provide a good source of information for qualitative studies such as in correlation within reservoirs throughout the field.

Fourteen analogue wireline logs consisting of gamma ray, sonic, spontaneous potential, resistivity, density and porosity were supplied by PETRONAS Petroleum Research & Scientific Services Sdn. Bhd. were used in this study. Most of these logs were acquired in the 60's and 70's and some e.g. sonic has to be digitised in order to carry out further study. Their distribution in the area is shown in Figure 1.

## CYCLE BOUNDARIES AND AGE DETERMINATION

The sedimentary cycle boundaries were determined from the wireline data. These cycle boundaries were later transferred to seismic sections, the mappable reflectors representing the cycle boundaries were later picked. Including the sea bed, nine horizons were identified and correlated with wireline logs. Two way time/depth relationship are listed in Table 1 (based on check shot data of two wells located in the survey area).

These picked boundaries were further checked by correlating them to the uplifted area where they normally became erosional unconformities. Once the cycle boundaries were confidently picked, correlations were made throughout the study area. The age of the sedimentary boundaries could then be inferred from the Baram Delta stratigraphic scheme calibrated with absolute time scale of Harland *et al.* (1989) (Fig. 2).

## SEDIMENT THICKNESS DETERMINATION FROM WELL LOGS

Gamma ray or spontaneous potential logs whichever available were used to distinguish between sandstone dominated and shale dominated zones. In this study, boundaries among sandstone, shaly sand and shale facies were marked in nine selected wells (2, 4, 5, 7, 8, 9, 18, 24, and 32).

Percentages of each facies penetrated in the

nine wells for Cycle VII, Cycle VI Upper, Cycle VI Middle, Cycle VI Lower, and Cycle V Upper are shown in Figure 3. Readings for Cycle VII and Cycle V Upper were not complete. For Cycle VII the upper boundary was not exactly known, and readings were taken from the uppermost (shallowest) readings of the well logs. The lower boundary of Cycle V Upper was also not known, so readings were taken at the deepest readings penetrated by the wells.

The average results of the nine wells are shown in the bottom right hand corner of the figure. Results show that the field is sandstone dominated (42%). Thicker reservoir sands occur in Cycle VI Lower which is about 46%. The thickness of the reservoir sands also increases toward north and northwest directions. This reflects that the subsidence of the area increases in the north and northwest directions.

## POROSITY/DEPTH RELATIONSHIP

Sand and shale are distinguished on spontaneous potential logs by using a dividing line offset 25% from the shale base line (Fig. 4). In the absence of spontaneous potential logs or when the spontaneous potential curve is featureless, gamma ray logs were used in distinguishing sands from shales.

The porosity/depth relationships for sand and shale were computed from well logs. Most of the wells were logged in the 60's and 70's, and not *all* logs have complete density logging. So density and electrical logs from selected wells were used to generate usable empirical porosity/depth relationships for sand and shale.

The corresponding sand and shale porosities were computed from density logs, assuming a grain density of 2.65 g/cm$^3$ (Schlumberger, 1987). Figure 5(A) shows the porosity/depth relationship for shale in Well 42. The porosity decreases with depth as expected due to an increase in compaction with depth. Overpressured shale can be identified from this plot which shows a sudden increase in porosity at a depth of about 2,100–2,300 m as shown in that figure.

Figures 5(B, C, D) show that the occurrence of overpressured shale as shown from sonic, density and resistivity plots of Well 42. The overpressured shale is also identified in Well 8 in as shown in

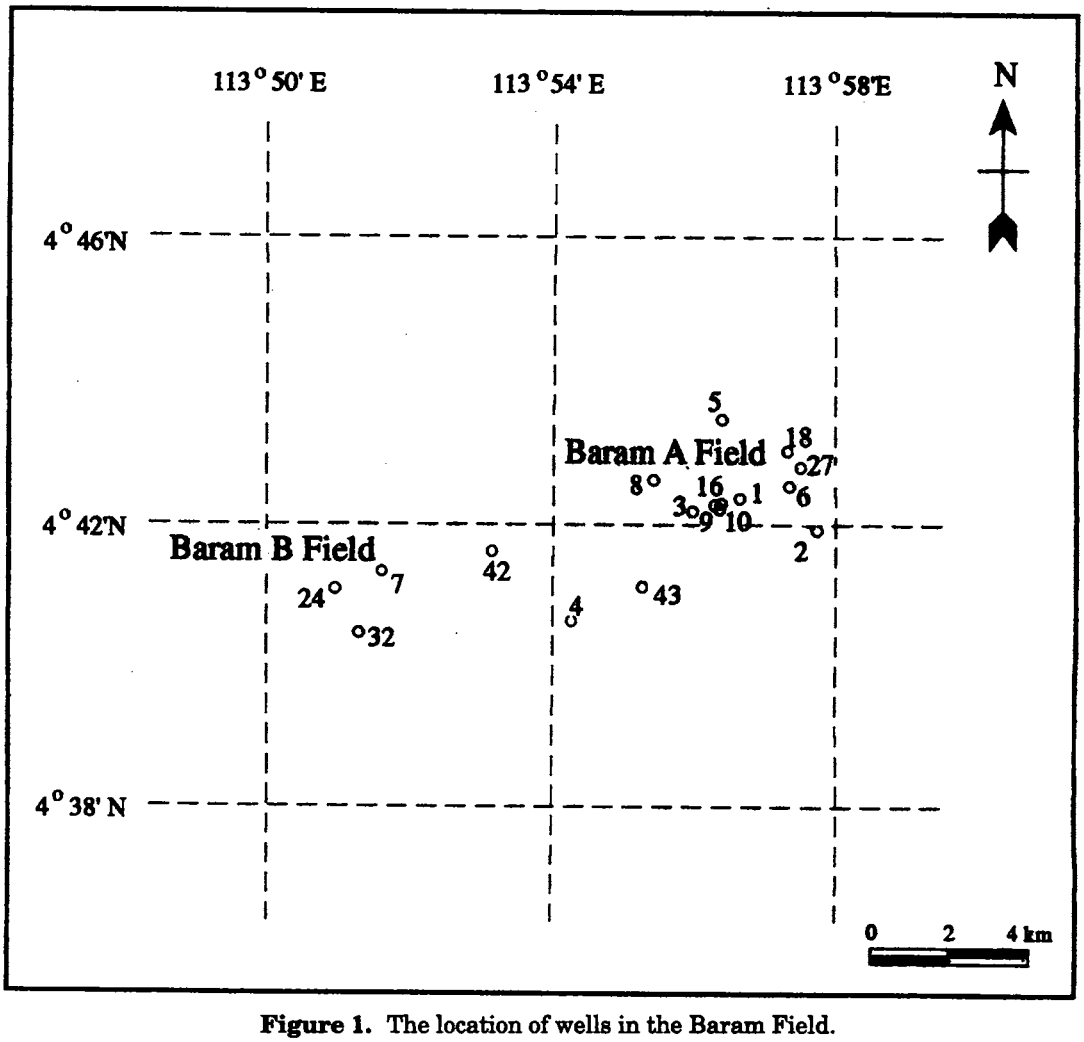


**Figure 1.** The location of wells in the Baram Field.

**Table 1.** Depth of identified horizons (metres) and two-way time (seconds) obtained from seismic sections and check shot data in well 43 as correlated from wireline logs in the study area.

| Well Name | Water Depth | Horizon 1 Base of Cycle VII | Horizon 2 Base of Cycle VI Upper | Horizon 3 Base of Cycle VI Middle | Horizon 4 Unconformity | Horizon 5 Base of Cycle VI Lower | Horizon 6 | Horizon 7 |
|---|---|---|---|---|---|---|---|---|
| 1 | 16.5 | 561.0 (0.62) | 870.4 (0.9) | 1,155.5 (1.1) | 1,323.2 | 1,689.0 (1.5) | 1,896.3 (1.67) | 2,225.6 (1.91) |
| 2 | 6.7 | 525.9 (0.6) | 878.1 (0.9) | 1,144.8 (1.12) | 1,274.4 | 1,750.5 (1.55) | 2,006 | 2,285.1 |
| 3 | 28.5 | 498.5 (0.57) | 911.6 (0.87) | 1,128.0 (1.08) | 1,301.8 | 1,734.8 (1.47) | 1,942.0 (1.66) | 2,191.5 (1.87) |
| 4 | 31.5 | 487.8 (0.55) | 812.5 (0.85) | 1,024.3 (1.0) | 1,253.0 | 1,600.6 (1.46) | 1,843.0 | 2,084.5 |
| 5 | 43.5 | 603.7 (0.66) | 939.0 (0.97) | 1,253.0 (1.2) | 1,378.0 | 1,862.8 (1.6) | 2,057.9 | 2,347.6 |
| 6 | 16.5 | 562.5 (0.63) | 914.6 (0.94) | 1,211.8 | 1,321.6 | 1,769.8 (1.56) | 2,034.1 | 2,332.3 |
| 7 | 55.5 | 591.5 (0.65) | 940.5 (0.96) | 1,143.3 (1.12) | 1,251.5 | 1,734.8 (1.54) | 2,016.8 | 2,336.9 |
| 8 | 37.5 | 530.5 (0.6) | 891.8 (0.92) | 1,115.8 (1.1) | 1,311.0 | 1,762.2 (1.56) | 1,975.6 (1.67) | 2,295.7 (1.86) |
| 9 | 22.5 | 539.6 (0.61) | 868.9 (0.9) | 1,131.1 (1.1) | 1,259.1 | 1,730.2 (1.53) | 2,023.5 | 2,349.1 |
| 10 | 31.5 | 539.6 (0.6) | 899.4 (1.04) | 1,135.7 (1.27) | 1,295.7 | 1,768.3 (1.66) | 2,086.9 | 2,300.3 |
| 18 | 19.5 | 582.3 (0.65) | 893.3 (0.93) | 1,251.5 (1.22) | 1,378.0 | 1,786.0 (1.57) | 2,067.0 | 2,314.0 |
| 23 | | 779.0 (0.82) | 1,167.7 (1.14) | 1,504.6 (1.39) | | 2,213.4 (1.8) | | |
| 24 | 49.5 | 591.5 (0.65) | 951.2 (0.97) | 1,167.7 (1.15) | 1,326.2 | 1,793.9 (1.57) | 2,076.2 | 2,368.9 |
| 27 | | | | | | 1,766.8 | 2,022.9 | 2,318.6 |
| 32 | 52.5 | 515.2 (0.58) | 862.8 (0.89) | 1,179.9 | 1,384.1 | 1,772.0 | | |
| 42 | 49.4 | 542.7 (0.61) | 914.6 (0.94) | 1,137.2 (1.12) | 1,301.8 | 1,759.1 (1.56) | 2,045.7 (1.69) | 2,335.4 (1.9) |

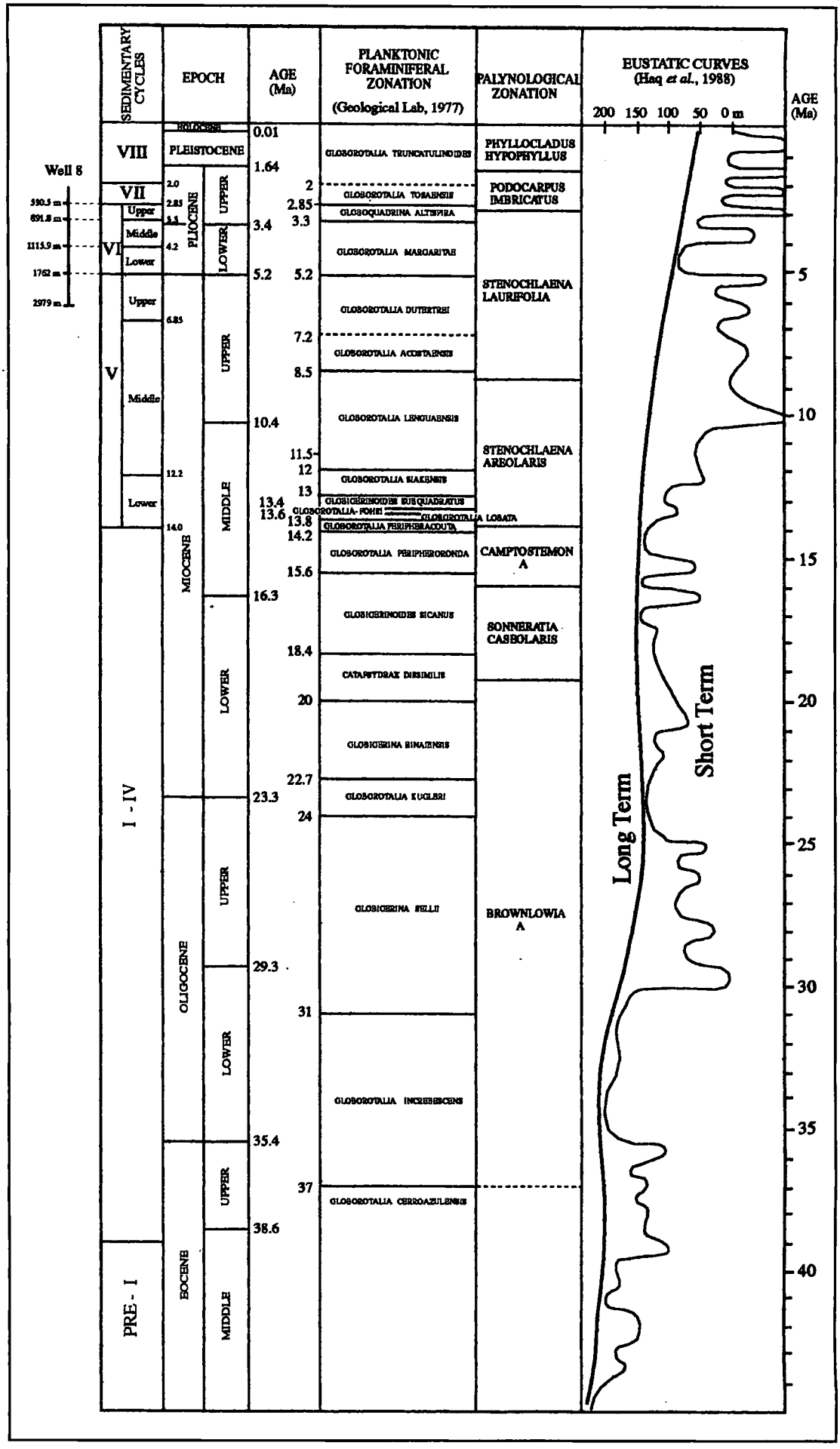


**Figure 2.** The biostratigraphic divisions of Tertiary rocks of the Baram Delta area and their relationship to Tertiary sea-level curve of Haq *et al.* , 1988 and GTS89 definitive time scale of Harland *et al.* , 1989 (modified from James, 1984).

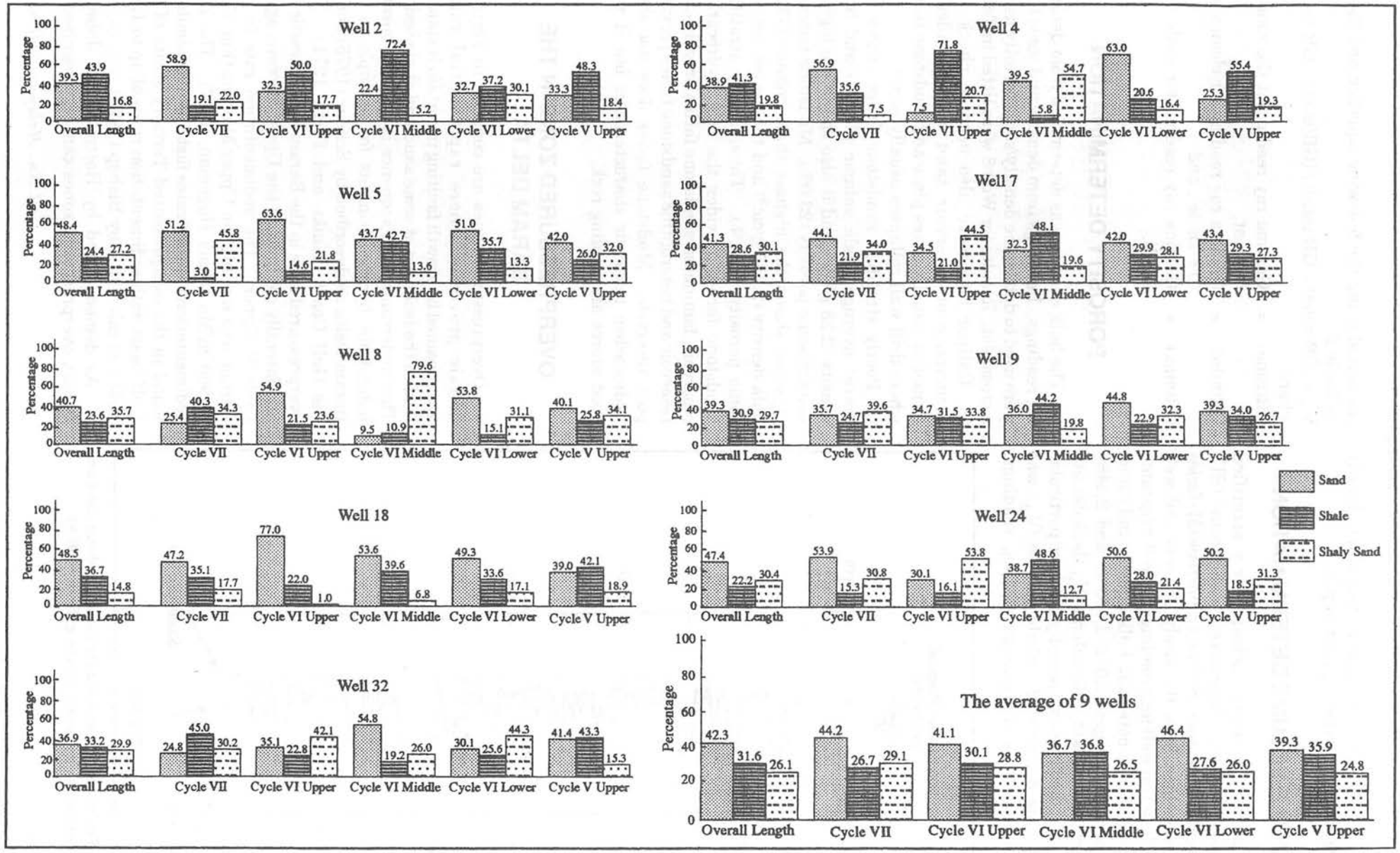


**Figure 3.** The percentage of sand, shale and shaly sand from 9 wells and their averages.

Figures 6(A, B, C) for sonic transit time, density and resistivity plotted against depth.

## SHALE VOLUME DETERMINATION

Four sedimentary facies; poorly stratified sandstone (Sps), laminated sandstone (Sl), heterolithic sandstone (Sm) and mudstone (M) facies were identified from the study of cores and well logs. Based on well logs readings of Well 8 (gamma ray/spontaneous potential, bulk density and sonic) at two depth ranges (2,012–2,100 m and 2,448–2,558 m), averages of shale volume ($V_{sh}$) bulk density ($rho_B$) and density/sonic porosity for these particular facies were determined. Shale volume ($V_{sh}$) was determined from the gamma ray log readings, calculated using the following equation and listed in Table 2:

$V_{sh}$ = [GR(zone) – GR(min)] / [GR(max) – GR(min)]

where;

GR(zone) = Gamma ray reading at the zone of interest,

GR(min) = Gamma ray reading for clean sand (0% shale), and

GR(max) = Gamma ray reading for shale (0% sand).

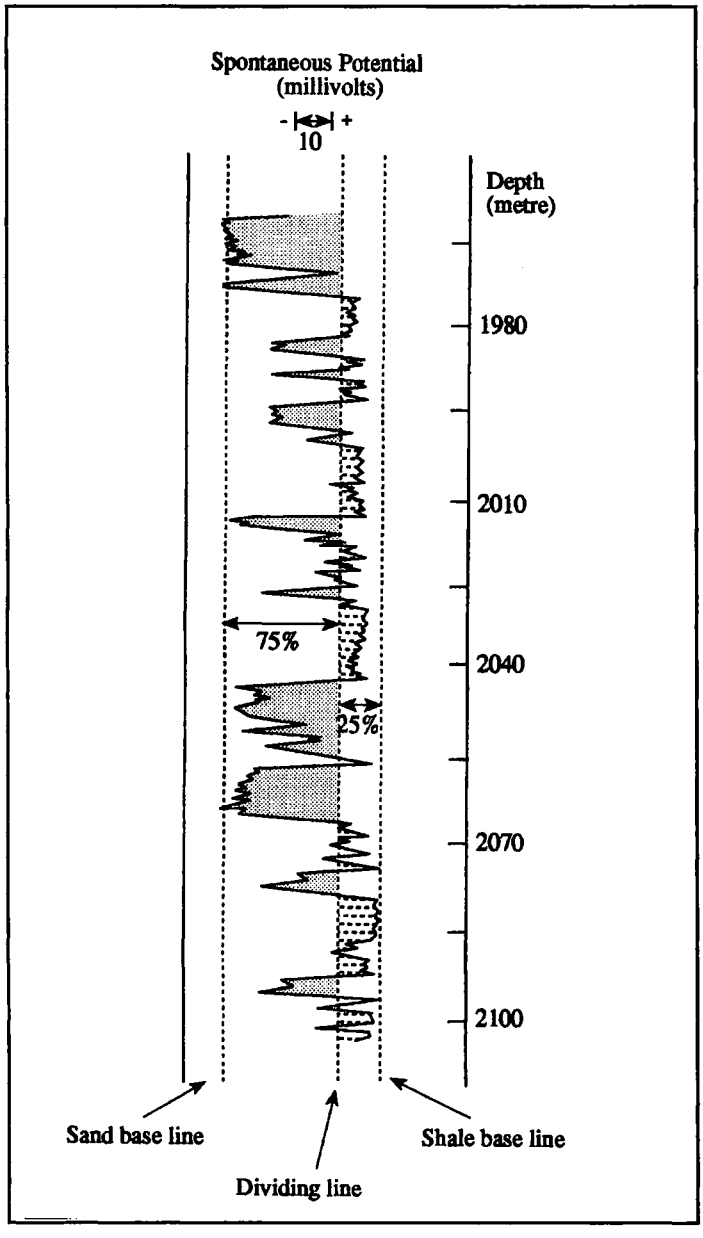


**Figure 4.** The dividing line used for distinguishing sand and shale on spontaneous potential logs (e.g. from Well 8).

## POROSITY DETERMINATION

The bulk density was determined from density log readings. Readings from density and sonic logs were used to determine density/sonic porosity using a cross plot. Results for Well 8 were listed in Table 2. Caliper logs were also used to check the occurrence of reservoir sand where mudcake formation usually takes place and mudstone facies where drill wall collapses usually occur.

Poorly stratified sandstone facies shows the lowest average shale volume (11.5%) and bulk density (2.28 g/cm$^3$) and it also shows the highest density/sonic porosity (23.0%). Mudstone facies as expected shows the highest shale volume (77%), bulk density (2.385 g/cm$^3$) and the lowest density/sonic porosity (19.1%). Thus, poorly stratified sandstone facies provides the best hydrocarbon reservoir, laminated sandstone facies provides fair reservoir and heterolithic sandstone facies provides poor reservoir. Mudstone facies does not show hydrocarbon reservoir characteristics but it is a good source and sealing rock.

## OVERPRESSURED ZONE IN THE BARAM DELTA

Overpressured zones are common in Tertiary deltaic provinces where rapid burial rates, accompanied by growth faulting in certain instances, lead to the isolation of some sand and shale bodies. This undercompacted sequence is an unfavourable habitat for hydrocarbons as for example in the Baram Delta as described by Schaar (1976) and in the Gulf Coast (Timko and Fertl, 1971). The overpressured zone in the Baram Field is vertically and laterally confined to the Upper Miocene age of Cycle V Upper. The sedimentation rate in the Baram area was high in Upper Miocene (Fig. 7) up to 900 m/Ma (Hans Hageman, 1987). The high sedimentation rate indicates fast burial as similarly found in the overpressured Tertiary strata of the Gulf Coast with sedimentation rates of up to 1,500 m/Ma as calculated by Bishop (1979).

As demonstrated by Hottman and Johnson (1965), overpressured zones can be recognised by

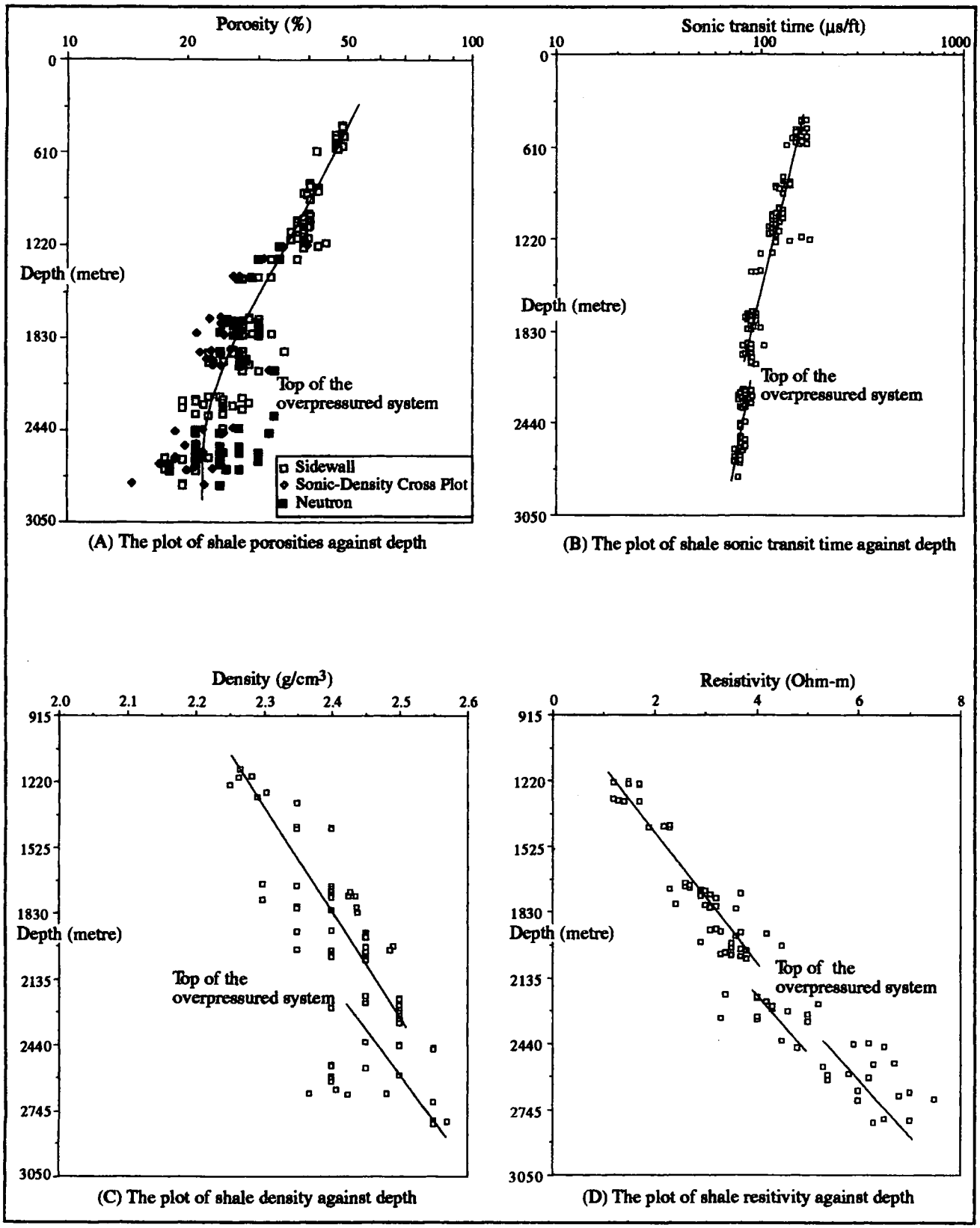


**Figure 5.** Plots of porosities, sonic interval transit time, density and resistivity against depth in Well 42.

changes in the physical properties, particularly as reflected by sonic, resistivity and bulk density logs. These changes, in certain areas however do not always show the occurrence of an overpressured zone (for example Carstens and Dypvik, 1981), but it seems applicable to the Baram Field overpressures as shown by Figures 5 and 6.

## THE ECONOMIC OF OVERPRESSURED ZONE

Overpressures have been found to have the retarding effect on the maturation of organic-matter and petroleum generation. The retarding effect of overpressures on organic-matter maturation has

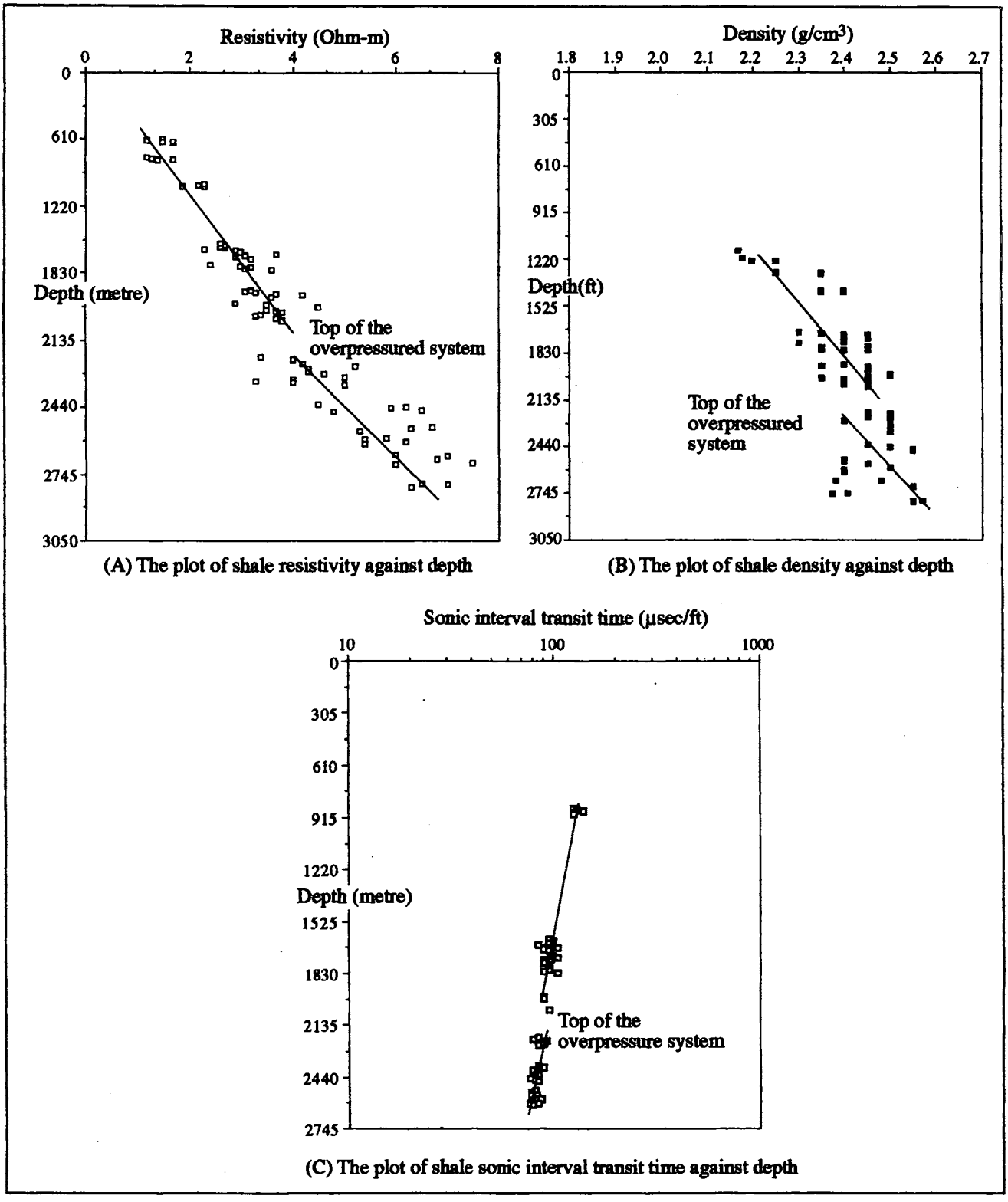


**Figure 6.** Plots of resistivity, density and sonic interval transit time against depth in Well 8.

**Table 2.** Average values for shale volume (%), bulk density (g/cm³) and density/sonic porosity (%) for various sedimentary facies as correlated with core in well 8.

| | Shale Volume (%) – Vsh (%) | | | Bulk Density (g/cm³) | | | Density/Sonic Porosity (%) | | |
|---|---|---|---|---|---|---|---|---|---|
| | 2,012–2,100 m | 2,448–2,558 m | Average | 2,012–2,100 m | 2,448–2,558 m | Average | 2,012–2,100 m | 2,448–2,558 m | Average |
| Sps | 8.0 | 15.0 | 11.5 | 2.31 | 2.25 | 2.280 | 24.5 | 21.5 | 23.00 |
| Sl | 17.0 | 21.0 | 19.0 | 2.32 | 2.27 | 2.295 | 24.3 | 20.8 | 22.55 |
| Sm | 34.0 | 33.0 | 33.5 | 2.33 | 2.36 | 2.345 | 23.4 | 19.5 | 21.45 |
| M | 78.0 | 76.0 | 77.0 | 2.37 | 2.40 | 2.385 | 19.6 | 18.6 | 19.10 |

Sps — Poorly stratified sandstone facies
Sl — Laminated sandstone facies
Sm — Hetereolithic sandstone facies
M — Mudstone facies

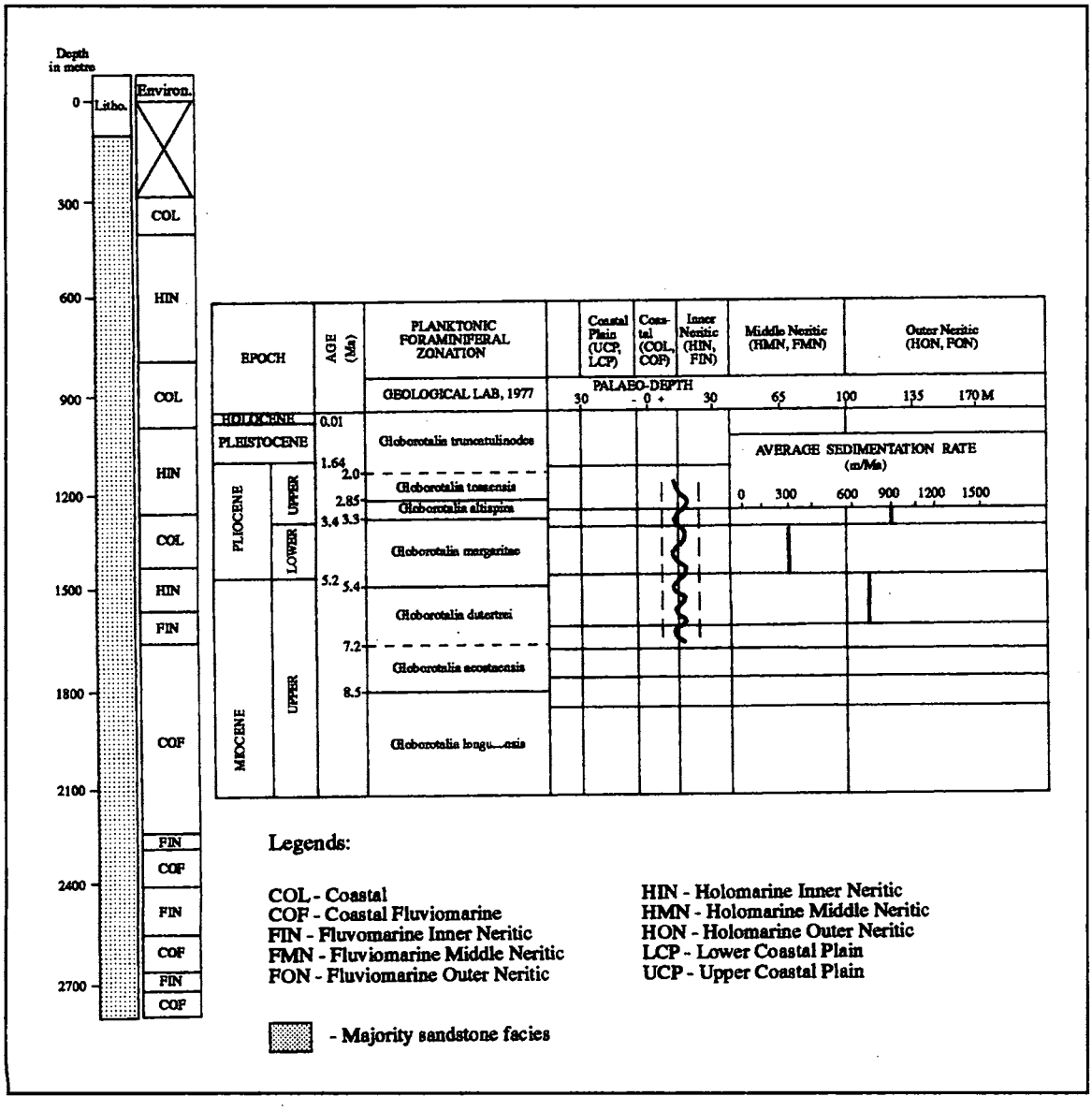


**Figure 7.** An example from a well in the Baram Province, stratigraphic log, palaeobathymetric curve and average sedimentation (modified from Hans Hageman, 1987).

been shown in the field by McTavish (1978) and in laboratory simulations (e.g. Price and Wenger, 1992). The overpressures retard organic maturation to level far lower than the level predicted from classical geochemical models (Hao *et al.*, 1995). Thus, need higher burial temperatures for maturation than expected. However, this retarding effect is not universal, indicating that this effect only occurs under certain conditions. Geochemical studies (outside the scope of this study) have to be carried out to show whether the retarding effect occurs in the overpressured zone of the study area.

The absence of hydrocarbons in the overpressured zone might be due to very early sealing and lack of generation within the present overpressured zone as suggested by Schaar (1976). It might be also due to very early sealing, generation of hydrocarbons within the present overpressured zone and subsequent leakage. The only hydrocarbons found in overpressured reservoirs in the Baram Delta are associated with inflation pressures. The inflated zones directly overlying the overpressured zones containing abundant hydrocarbons with a preference for gas relative to oil with increasing pressure gradient.

## GEOTHERMAL GRADIENT

The geothermal gradient for the Baram Field was calculated by plotting bottom-hole temperatures (BHT) against depth. No temperature corrections were applied for either topographic or uplift/erosion. The area itself has lower temperature gradient as compared to other economic provinces (Fig. 8). The temperature gradient plot of the area (Fig. 9) shows an average geothermal gradient of 1.75°C/100m. The gradient increases slightly at the top of the overpressured zone to about 2.79°C/100m at depth about 2,250 m. The temperature at the onset of the overpressure is approximately 70°C and increases linearly with depth, with maximum recorded temperature of about 94°C at 3,170 m.

## DISCUSSION

The geothermal gradient is proportional to the heat flow and inversely proportional to the thermal conductivity of the material in which the geothermal gradient is measured. Thermal conductivities of rocks with a similar mineral composition can be very different due to variations in saturating fluids (oil, gas, and water), porosity, and texture. The thermal conductivities are relatively sensitive to fluid and porosity because the conductivity of fluids is much lower than the conductivity of the rock matrix (Zierfuss, 1969). Because the overpressured zone contains an excessive amount of water, it tends to have a thermal conductivity lower than that in the normally pressured zone. If heat flows upward at a given rate, the geothermal gradient in the overpressured zone would become greater than that in the normal pressured zone. This is in agreement to what was reported by Schmidt (1973) in the Gulf Coast where there was an increase in the geothermal gradient over the top of the overpressured zone.

The lower thermal conductivity in the overpressured system appears to have been caused by the abnormally higher porosity within the overpressured shale facies from about 20 to 30% (Fig. 5). The abnormally high porosity and fluid volume associated with undercompaction, hydrocarbon generation, and/or clay dehydration result in a significant reduction of the thermal conductivity of the overpressured shale facies (Luo *et al.*, 1994).

Dickinson (1953) for example observed that within the overpressured zone onshore US Gulf Coast Tertiary strata the onset of abnormal pressures lies where sandstones constitute less than 5–10% of the rock sequence. In the Baram Field, sandstone forms about 50% of the strata within the upper part of the overpressured zone and decreases gradually to about 20% toward the lower part of the overpressured zone.

## CONCLUSIONS

The Baram Delta field is sandstone dominated, averaging 42.3% sand, 31.6% shale, and 26.1% shaly sand. The thickness of the reservoir sand increases towards north and northwest directions, suggesting subsidence increases in those directions (basinward). Rapid sedimentation rates in the area led to the formation of a overpressured zone at depth of about 2,100–2,300 m. The presence of this overpressured zoned was shown by wireline logs. This overpressured zone is an unfavourable habitat for hydrocarbons. The major temperature gradient change appears to occur at the position of the sudden increase in the shale porosity, the mineralogy change, the lithology change to dominantly shale sequence, and the increase in pressure.

## REFERENCES

BISHOP, R.S., 1979. Calculated compaction states of thick abnormally pressured shales. *American Association Petroleum Geologists Bulletin* 63(6), 918–933.

CARSTENS, H. AND DYPVIK, 1981. Abnormal formation pressure and shale porosity. *American Association Petroleum Geologists Bulletin* 65, 344–350.

DICKINSON, G., 1953. Geological aspects of abnormal reservoir pressures in Gulf Coast, Louisiana, USA. *American Association Petroleum Geologists Bulletin* 37(2), 410–432.

HANS HAGEMAN, 1987. Palaeobathymetrical changes in NW

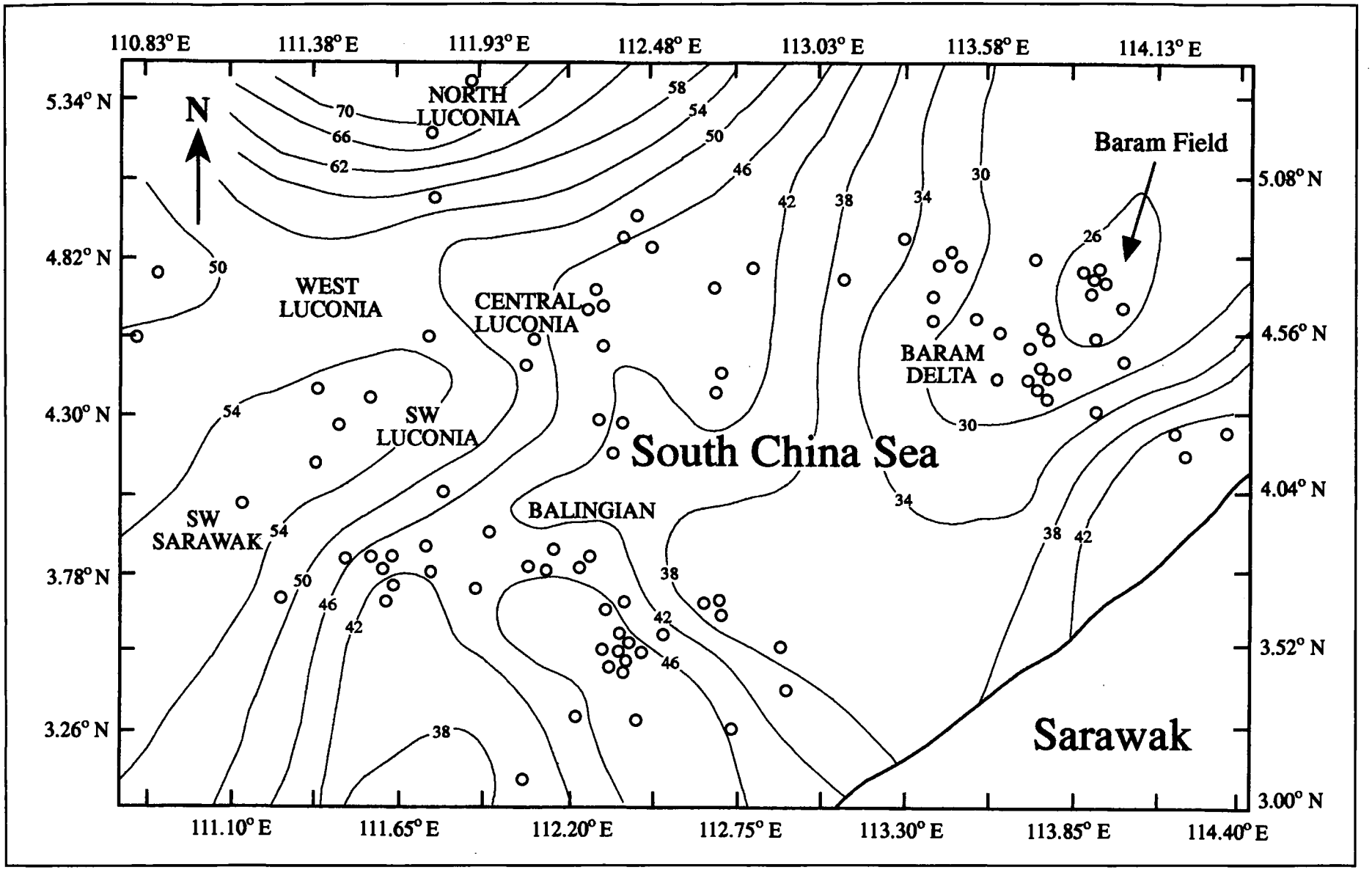


**Figure 8.** Areal distribution of the average geothermal gradient, offshore Sarawak (contour interval of 4°C/km). Circles represent data points (data provided by PETRONAS).

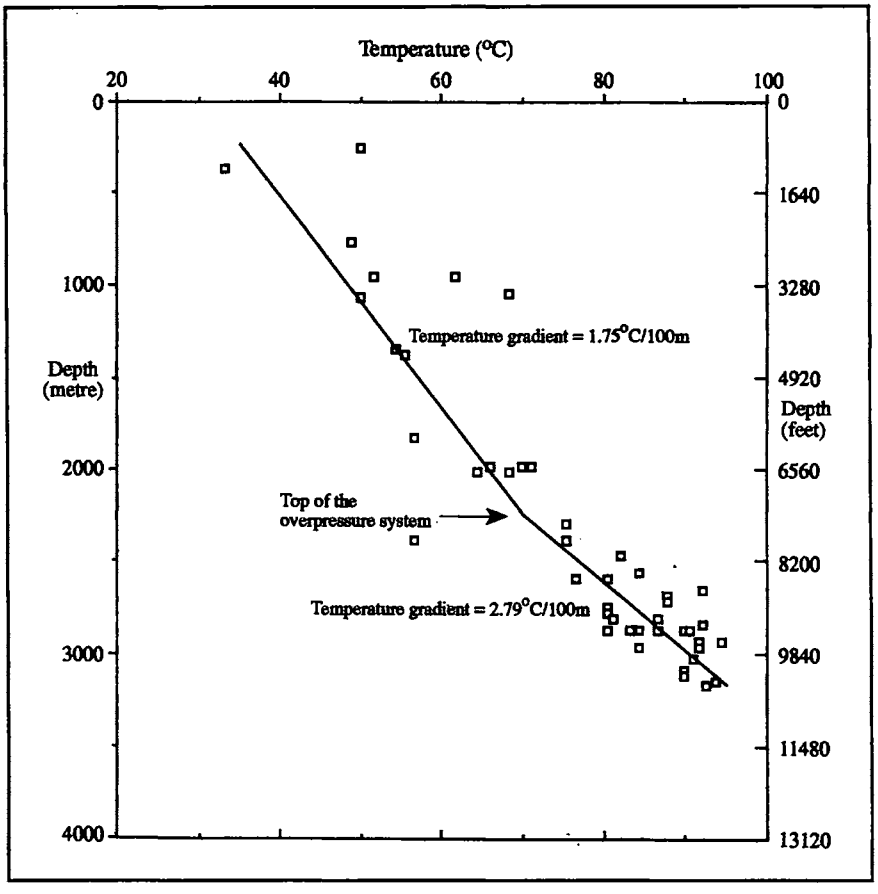


**Figure 9.** Well log temperatures taken from 15 wells showing the change in the temperature gradient at the boundary of the overpressured system.

Sarawak during the Oligocene to Pliocene. *Geological Society of Malaysia Bulletin* 21, 91–102.

HAO, F., YONGCHUAN, S., SITIAN, L. AND QIMING, Z., 1995. Overpressure retardation of organic-maturation and petroleum generation: a case study from the Yinggehai and Qiongdongnan Basins, South China Sea. *American Association Petroleum Geologists Bulletin* 79(4), 551–562.

HAQ, B.U., HARDENBOL, J. AND VAIL, P.R., 1988. Mesozoic and Cenozoic chronostratigraphy and cycles of sea-level change. *In:* Wilgus, C.K., Hasting, B.S., Kendall, C.G.S.C., Posamentier, H.W., Ross, C.A., and Wagoner, J.C.V. (Eds.), Sea-level changes an integrated approach. *Society of Economic Paleontologists and Mineralogists Special Publication* 42, 71–108.

HARLAND, W.B., ARMSTRONG, R.L., COX, A.V., CRAIG, L.E., SMITH, A.G. AND SMITH, D.G., 1989. *Geological Time Scale 1989.* Cambridge University Press, Cambridge, 263 p.

HOTTMAN, C.E. AND JOHNSON, R.K., 1965. Estimation of formation pressures from log-derived shales properties. *Journal of Petroleum Technology* 17, 717–722.

JAMES, D.M.D., 1984. *The geology and hydrocarbon resources of Negara Brunei Darussalam.* Muzium Brunei, 169 p.

LUO, M., BAKER, M.R. AND LEMONE, D.V., 1994. Distribution of generation of the overpressure system, Eastern Delaware Basin, Western Texas and Southern New Mexico. *American Association Petroleum Geologists Bulletin* 78(9), 1386–1405.

MCTAVISH, R.A., 1978. Pressure retardation of vitrinite diagenesis, offshore northwest Europe. *Nature* 271, 648–650.

PRICE, L.C. AND WENGER, L.M., 1992. The influence of pressure on petroleum generation and maturation as suggested by aqueous pyrolysis. *Organic Chemistry* 19(1–3), 141–159.

SCHAAR, G., 1976. The occurrence of hydrocarbon in overpressured reservoir of the Baram Delta (offshore Sarawak, Malaysia). *Proceedings Indonesian Petroleum Association*, 163–169.

SCHLUMBERGER, 1987. *Log Interpretation Charts.* Schlumberger Publication.

SCHMIDT, G.W., 1973. Interstitial water composition and geochemistry of deep Gulf Coast shales and sandstones. *American Association Petroleum Geologists Bulletin* 57(2), 321–337.

TIMKO, D.J. AND FERTL, W.H., 1971. Relationship between hydrocarbon accumulation and geopressure and its economic significance. *Journal of Petroleum Technology* 22, 923–930.

ZIERFUSS, H., 1969. Heat conductivity of some carbonate rocks and clay sandstones. *American Association Petroleum Geologists Bulletin* 53(2), 251–260.

*Manuscript received 1 October 1997*